Journal of Physics: Conference Series **514** (2014) 012049 doi:10.1088/1742-6596/514/1/012049

Evaluation of the scrape-off-layer plasma parameters by a horizontal reciprocating Langmuir probe in the COMPASS tokamak

M Dimitrova[1,3,4], Tsv K Popov[2], P Ivanova[3], E Vasileva[3], E Hasan[2,3], J Horáček[1], P Vondráček[1], R Dejarnac[1], J Stöckel[1], V Weinzettl[1], J Havlicek[1], F Janky[1] and R Panek[1]

[1]Institute of Plasma Physics, Academy of Sciences of the Czech Republic v.v.i., 3 Za Slovankou, 182 00 Prague 8, Czech Republic
[2]Faculty of Physics, St. Kl. Ohridski University of Sofia, 5 J. Bourchier Blvd., 1164 Sofia, Bulgaria
[3]Acad. E. Djakov Institute of Electronics, Bulgarian Academy of Sciences, 72 Tsarigradsko Chaussee, 1784 Sofia, Bulgaria

E-mail: dimitrova@ipp.cas.cz

Abstract. The scrape-off-layer (SOL) parameters in the COMPASS tokamak are studied by using a Langmuir probe mounted on a horizontal reciprocating manipulator. The radial profiles of the plasma potential, the electron energy distribution function and the electron densities are derived from the measured current-voltage probe characteristics by applying the first-derivative probe technique (FDPT). It is shown that close to the tokamak wall the electron energy distribution function is Maxwellian, while in the SOL, in the vicinity of the last closed flux surface and inside the confined plasma, the electron energy distribution function is bi-Maxwellian with a low-energy electron fraction dominating over a higher energy one. The radial profiles of the electron pressure and the parallel electron power flux density in COMPASS are also presented.

1. Introduction

The electric probes are simple plasma diagnostic tools allowing one to evaluate quickly and reliably the edge plasma parameters. In magnetized plasma, the interpretation of the electron part of the current-voltage (*IV*) characteristics above the floating potential still remains difficult [1] because the electron part of the *IV* characteristics is distorted due to the influence of the magnetic field.

In tokamaks, the assumption for a Maxwellian electron energy distribution function (EEDF) is generally valid. However, experimental evidence does exist suggesting non-Maxwellian distributions in tokamak SOL plasmas [2]. It is clear that the knowledge of the real EEDF is of great importance in understanding the underlying physics in SOL plasma. This fact notwithstanding, only a few experimental works have so far been reported devoted to the EEDF direct measurement. Our investigations on the CASTOR tokamak aimed at evaluating the real EEDF indicated a bi-Maxwellian

[4] To whom any correspondence should be addressed.

one in the edge plasma [3]. Recent probe measurements in the liquid lithium divertor area of the NSTX also showed a bi-Maxwellian EEDF [4].

In this paper we report results of measurements in the SOL made by a horizontal reciprocating probe in the COMPASS tokamak [5] with D-shaped plasma. The radial distribution of the plasma potential, the electron temperatures and densities are presented and discussed. The radial distributions of the electron pressure and the parallel electron power flux density in COMPASS are also presented.

2. The first-derivative Langmuir probe technique for evaluating the EEDF in tokamak edge plasma

The FDPT for evaluating the plasma parameters in tokamak edge plasma was published and discussed in detail in [3]. It was shown there that the electron current flowing to a cylindrical probe negatively biased by potential U is given by:

$$I_e(U) = -\frac{8\pi eS}{3m^2\gamma}\int_{eU}^{\infty}\frac{(W-eU)\,f(W)dW}{\left[1+\frac{(W-eU)}{W}\psi(W)\right]}, \tag{1}$$

where W is the electron energy; e, m and n are the electron charge, mass and density; S is the probe area; U is the probe potential with respect to the plasma potential U_{pl} ($U = U_p - U_{pl}$). The geometric factor γ assumes values in the range of $0.71 \le \gamma \le 4/3$.

Here $f(W)$ is the isotropic EEDF normalized by:

$$\frac{4\pi\sqrt{2}}{m^{3/2}}\int_0^{\infty} f(W)\sqrt{W}\,dW = \int_0^{\infty} f(\varepsilon)\sqrt{\varepsilon}\,d\varepsilon = n. \tag{2}$$

In the presence of a magnetic field B at low gas pressures, the diffusion parameter $\psi = \psi(W, B)$ depends on the Larmor radius $R_L(W,B)$, as well as on probe size and orientation with respect to the magnetic field. As it was shown in [3], for cylindrical probes oriented perpendicular with respect to the magnetic field the diffusion parameter can be written as:

$$\psi_{\perp}(W,B) = \frac{R\ln\left(\frac{\pi L'}{4R}\right)}{16\gamma R_L(W,B)}, \tag{3}$$

where L' is the characteristic cross-section size of the turbulent structures (blobs), R is the radius of the probe.

As the magnetic field intensity increases, so does the value of the diffusion parameter. When $\psi(W,B) >> 1$ **(high value of the magnetic field *B*)**, the EEDF is represented by the first derivative of the electron probe current, as was shown in [3,6,7]:

$$f(\varepsilon) = \frac{3\sqrt{2\mathrm{m}\gamma}}{2e^3S}\frac{\psi}{U}\frac{dI_e}{dU}. \tag{4}$$

Note that in equation (4) the diffusion parameter is inversely proportional to the square root of the energy. This will cause the parameter to diverge at small energies and can cause an artifact in the resulting

distribution function. This artifact in the range from zero to the value of the electron temperature (on energy scale) is due to the mathematical approach rather than to physical phenomena [1,3].

3. Langmuir probe measurements in the COMPASS tokamak edge plasma

To diagnose the edge plasma and the SOL in the horizontal direction in the COMPASS tokamak, the *IV* characteristics were measured by using a reciprocating Langmuir probe. The graphite cylindrical probe tip (length 1.5×10^{-3} m and diameter 8×10^{-4} m) was placed perpendicular to the magnetic field lines. Before the shot, the probe was moved to a chosen initial position with respect to the center of the tokamak chamber and, in synchronization with the shot onset, started a fast reciprocation towards the last closed flux surface (LCFS) and back. The maximum extension of the reciprocating probe motion was 0.06 m.

A series of reproducible ohmic discharges in hydrogen with D-shape cross-section plasma were performed. We present below results from shot #3908, which is typical for the series. The toroidal magnetic field was 1.15 T. The measurements were performed during the steady-state phase of the discharge at a low loop-voltage (about 1.5 V), a constant plasma current of 170 kA and a line average electron density of 8.3×10^{19} m^{-3}. The position of the horizontal reciprocating probe (HRP) versus time is presented in figure 1. The red line indicates the probe position when the probe signal is collected (probe extension 0.04 m). In the same figure, the dashed line shows the position of the LCFS in the plasma, derived from the magnetic reconstruction.

The probe was biased with respect to the tokamak chamber wall by a triangular voltage $U_p(t)$ at a frequency of 1 kHz supplied by a KEPCO 100-4M power supply. The ramp-up/ramp-down phases lasted 0.5 ms, so that the probe could be assumed stationary in space during each sweep cycle. The probe potential and the probe current versus time were recorded by the tokamak Data Acquisition System. Thus, we could construct the *IV* characteristics at different probe positions and, using the FDPT, evaluate the real EEDF. In the far SOL (probe positions in the range 0.771 – 0.751 m) it appears to be Maxwellian. When going deeper into the plasma (probe positions in the range 0.751 – 0.731 m), the nature of the EEDFs measured changes: Besides the predominant low-energy fraction, a fraction of electrons with higher energy appears in the electron energy distribution function. In this case, the non-Maxwellian EEDF can be approximated by a bi-Maxwellian one – i.e., by a sum of two Maxwellian EEDF for two different temperatures. An example of a bi-Maxwellian EEDF measured at

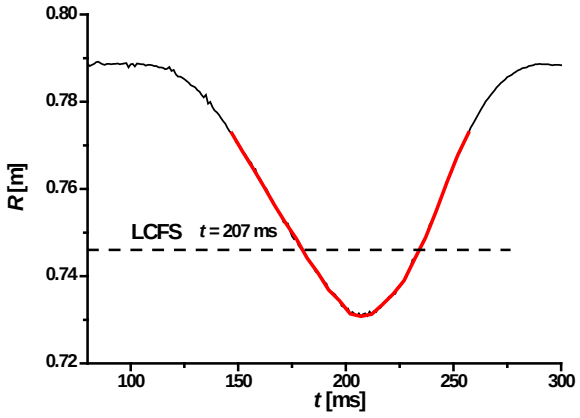

Figure 1. Position R of the HRP tip with respect to the tokamak chamber center versus time. The red line indicates the probe position when the probe signal is collected. The LCFS is indicated by a dashed line.

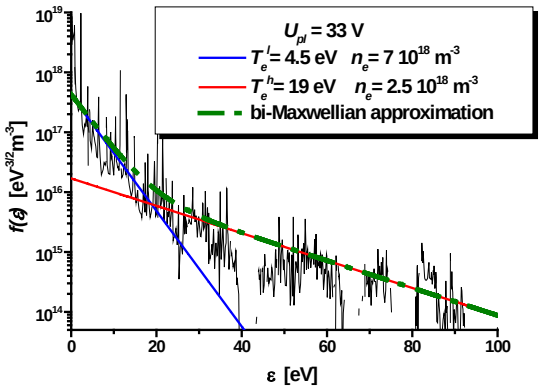

Figure 2. Experimental EEDF (black line) and the sum of the model ones for two electron temperatures (dashed dotted line). Shot #3908, probe position 0.731 m from the tokamak center.

the deepest probe position (0.731 m from the tokamak center) is presented in figure 2. The low-temperature electron group (blue line, $T_e^l = 4.5$ eV) has a density higher than that of the high-temperature one (red line, $T_e^h = 19$ eV). The electron densities were calculated by using equation (2).

4. Results and discussion

Figure 3 shows the radial distribution (with respect to the position of the LCFS) of the electron temperature – the triangles represent the temperature of the more populated low-energy electron fraction, while the squares, the temperature of the suprathermal electrons in the bi-Maxwellian EEDF. The dots indicate the temperature of the Maxwellian EEDF. The position of the LCFS evaluated by EFIT is indicated in all figures by a dashed line.

We should point out that more detailed theoretical and experimental investigations must be performed to clarify the origin of the low-energy fraction in the bi-Maxwellian EEDF. In [4], a "heuristic model" accounting for the inelastic collision effects (i.e. excitation and ionization of neutral hydrogen) is proposed to explain this EEDF feature. Indeed, the energy balance of the reaction $\mathrm{H} + \mathrm{e} \rightarrow \mathrm{H}^+ + 2\mathrm{e}$ for electrons with energy higher by 10 – 15 eV than the energy of ionization (13.6 eV) is in agreement with the energy of the low-temperature electrons registered. The values of the rate coefficient [8] for electron temperatures in the range 15 – 20 eV are close to the maximum. Performing a detailed energy balance necessitates that ionization through neutral hydrogen excited states be taken into account as well. On the other hand, the energy of the electrons in the far SOL is ~5 eV and the most probable reactions are dissociation with threshold of 4.5 eV and excitation. The behavior of the electron temperature spatial distribution at the vicinity of the separatrix can be explained by the plasma turbulence and non-local kinetic effects [9,10,11].

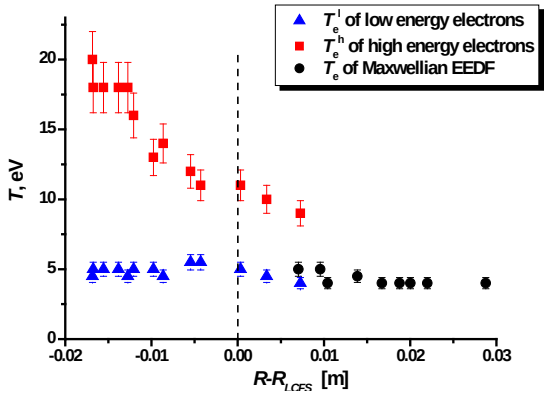

Figure 3. Radial distribution of the electron temperature T_e for shot #3908.

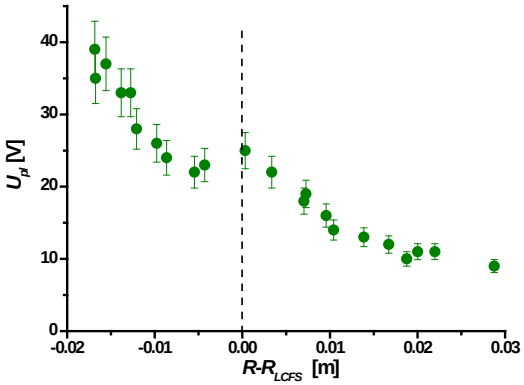

Figure 4. Radial distribution of the plasma potential for shot #3908.

The radial distribution of the plasma potential is presented in figure 4. The dots show the values evaluated by the FDPT.

In figure 5, the electron densities evaluated are represented by the same symbols as used in figure 3. Figure 6 shows the ratio between the electron densities of the two electron groups. The solid symbols represent the data for the reciprocating probe motion from its initial position to its maximum extension. The empty symbols illustrate the data measured during the backward probe motion. It is seen that the density of the high-energy electron group increases from 15% to 43% within a few millimeters after the LCFS.

Using the results for the electron temperatures and densities obtained by probe measurements, we can also calculate other plasma parameters. Figure 7 presents the radial distribution of the electron pressure p_e, namely, $p_e = n_l k T_e^l + n_h k T_e^h$, where the EEDF is by-Maxwellian, and $p_e = n_M k T_e^M$ for

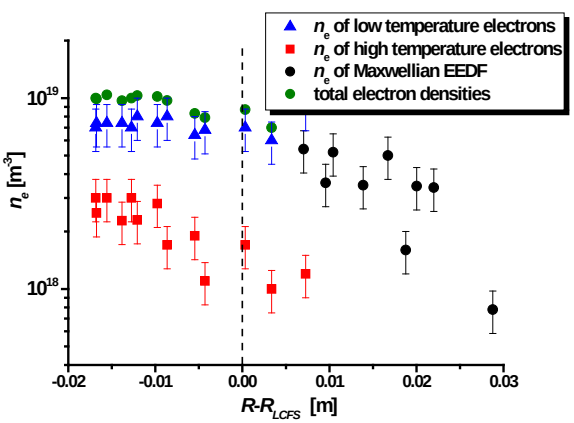

Figure 5. Radial distribution of the electron densities n_e for shot # 3908.

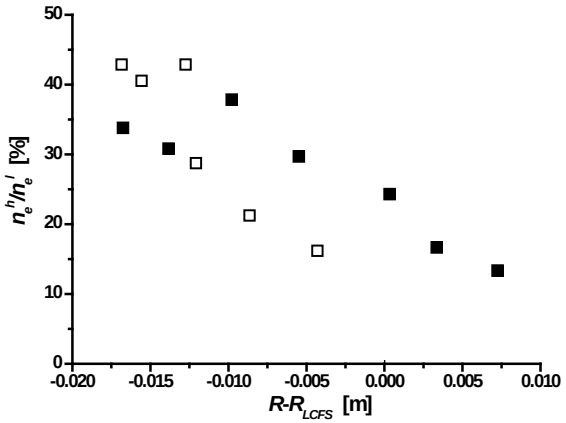

Figure 6. Ratio between densities of the high and the low temperature electron groups.

a Maxwellian case. The values of T in these equations are expressed in Kelvin and k is the Boltzmann constant. It is seen that, within the experimental error, the electron pressure radial distribution has an exponential behavior versus the radial position.

Figure 8 presents the results from the calculations of the parallel electron power flux density [8] $Q_{\parallel}^{e} = \frac{7}{2} c_s p_e$. In the SOL, the power flux density decreases exponentially as $Q_{\parallel}^{e} = Q_0 \exp\left(-\left(R - R_{LCFS}\right)/\lambda_q\right)$, where the decay length λ_q = 0.015 m and the power flux density at the LCFS Q_0 = 0.9 MW/m^2 (the solid line in figure 8).

Such a profile shape is regularly observed when other probe techniques are used and in most of tokamaks [12]. This is usually interpreted in terms of turbulent structures (blobs) transporting plasma radially away from the LCFS with a roughly constant speed, with the plasma loosing both its density and temperature in parallel with the magnetic field lines by acoustic streaming (determined by the ion sound velocity, or the parallel pressure gradient).

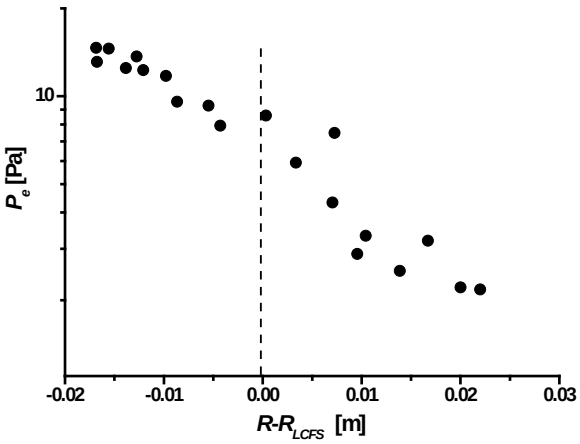

Figure 7. Radial distribution of the electron pressure for shot # 3908.

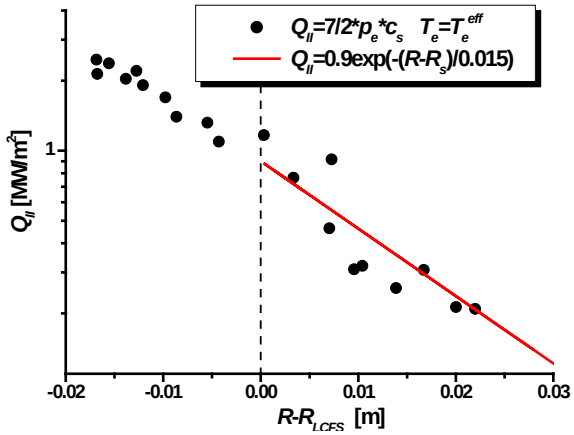

Figure 8. Radial distribution of the parallel electron power flux density for shot # 3908.

5. Conclusions

The SOL parameters in the COMPASS tokamak are studied by using a horizontal reciprocating Langmuir probe. Data for the radial distribution of the plasma potential, the electron energy distribution function and the electron densities are derived from the measured current-voltage probe characteristics by applying the first-derivative probe technique. It is shown that close to the wall of the tokamak chamber the energy distribution function of the electrons is Maxwellian, while in SOL, around the last closed flux surface and inside the confined plasma, the electron energy distribution function is bi-Maxwellian with a low energy electron fraction dominating over the higher energy one. The radial profiles of the electron pressure and the parallel electron power flux density in the COMPASS tokamak are also presented.

Acknowledgements

This research has been supported by the European Community under the contract of Association between EURATOM/IPP.CZ and EURATOM/INRNE.BG; Bulgarian Science Fund through the Association EURATOM-INRNE, International Atomic Energy Agency (IAEA) Research Contract No 17125/R0 as a part of the IAEA CRP F13014 on "Utilisation of a Network of Small Magnetic Confinement Fusion Devices for Mainstream Fusion Research" and 5th IAEA Joint Experiment, by the JOINT RESEARCH PROJECT between Institute of Plasma Physics v.v.i., AS CR and Institute of Electronics BAS BG, the grant project GA CR P205/12/2327 and by MSMT Project # LM2011021.

References

[1] Popov Tsv K, Ivanova P, Dimitrova M, Kovačič J, Gyergyek T and Čerček M 2012 *Plasma Sources Sci. Technol.* **21** 025004 A
[2] Dejarnac R, Gunn J P, Stöckel J, Adámek J, Brotánková J and Ionita C 2007 *Plasma Phys. Control. Fusion* **49** 1791-1808
[3] Popov Tsv K, Ivanova P I, Stockel J and Dejarnac R 2009 *Plasma Phys. Control. Fusion* **51** 065014
[4] Jaworski M A, Bell M G, Gray T K, Kaita R, Kallman J, Kugel H W, LeBlanc B, McLean A G, Sabbagh S A, Soukhanovskii V A, Stotler D P and Surla V 2012 *Fusion Engin. Design* **87** 1711-18
[5] Pánek R, Bilyková P, Fuchs V, Hron M, Chráska P, Pavlo P, Stockel J, Urban J, Weinzettl V, Zajac J and Zacek F 2006 *Czechoslovak J. Phys.* **56**/2 B125–137
[6] Arslanbekov R R, Khromov N A and Kudryavtsev A A 1994 *Plasma Sources Sci. Technol.* **3** 528-38
[7] Demidov V I, Ratynskaia S V and Rypdal K 2002 *Rev. Sci. Instrum.* **73** 3409-39
[8] Stangeby P C 2000 *The Plasma Boundary of Magnetic Fusion Devices (Series in Plasma Physics)* (IOP)
[9] Tskhakaya D, Jachmich S, Eich T, Fundamenski W and JET EFDA Contributors 2011 *J. Nuclear Mater.* **415** S860-4
[10] Chodura R 1992 *Contr. Plasma Phys.* **32** 219-30
[11] Batishchev O V, Krasheninnikov S I, Catto P J, Batishchev A A, Sigmar D J, Xu X Q, Byers J A, Rognlien T D, Cohen R H, Shoucri M M and Shkarofskii I P 1997 *Phys. Plasmas* **4** 1672-80
[12] Horacek J, Pitts R A, Vondracek P, Panek R, Goldston R, Stangeby P C, Kocan M, Janky F, Havlicek J and Arnoux G 2013 Heat flux deposition on ITER-like HFS limiter on tokamak COMPASS *Presented at 18th ITER ITPA Div-SOL meeting* (March.2013 Hefei China)